Topology controlled frustrated solid state of ionic liquids without a detectable melting transition

Satoshi Okamoto

satoshi.okamoto.fv@riken.jp

RIKEN https://orcid.org/0009-0008-3901-6882

Justin Llandro

Sumitomo Chemical Co., Ltd.

Article

Keywords:

Posted Date: August 7th, 2026

DOI: https://doi.org/10.21203/rs.3.rs-10321809/v1

Additional Declarations: Yes there is potential Competing Interest. S.O. is an inventor on a patent application related to the materials described in this work. All other authors declare no competing interests.

Abstract

Meta-linked polymer topology can stabilize a frustrated solid state of ionic liquids that retains long-range order without any detectable melting transition. Using phase-change polymerization of poly(metabenzamide) (pMBA) in BMIM–PF6, we generate a confined ionic phase that exhibits sharp, thermally reversible diffraction features up to 320°C, while differential scanning calorimetry shows no melting transition between − 40°C and 350°C. Electrochemical impedance spectroscopy further reveals finite ionic conductivity at 30°C, indicating that the ordered confined state is not fully dynamically arrested. Control experiments show that a para-linked analogue does not stabilize the ordered ionic phase, whereas an amorphous meta-linked host, poly(metaoxybenzamide) (pMOB), reproduces similar behaviour without requiring a crystalline polymer lattice. These observations identify topology-controlled chemical confinement as the governing principle and support a picture in which polymer crystallization transfers a frustration-dominated energy landscape to the confined ionic liquid. Our findings demonstrate that polymer architecture can decouple structural order from dynamical arrest, providing a design principle for engineering ordered ionic materials with independently tunable structural and transport properties.

Introduction

Ionic liquids (ILs) have attracted considerable interest owing to their negligible vapour pressure, wide electrochemical windows, and intrinsic ionic conductivity.[1–3]

A defining characteristic of ILs is their resistance to crystallization, arising from structural asymmetry, conformational flexibility, and frustrated packing interactions, which typically lead to disordered liquid or glassy states rather than long-range ordered crystals.[2, 4–6]

In such disordered states, structural fluctuations enable efficient ionic motion.[7–9]

In contrast, in crystalline solids, ionic motion is generally suppressed because ions are localized at periodic lattice sites and transport occurs only through thermally activated or defect-mediated processes.[7–9]

This fundamental relationship has led to the widely accepted view that crystallinity and ionic mobility are intrinsically incompatible.

This trade-off is also well recognized in solid-state ionic conductors, including lithium-ion battery electrolytes, where high crystallinity often limits ionic transport.[7, 10]

This apparent trade-off between structural order and dynamical freedom is not unique to ionic systems, but represents a more general feature of condensed matter.

More generally, confinement has been widely recognized as a powerful strategy to alter phase behaviour across a broad range of molecular systems, including water, hydrocarbons, and polymers.

In these systems, nanoconfinement and interfacial effects can induce crystallization, stabilize metastable phases, and shift melting or freezing transitions.[11–14]

For example, nanoconfined water exhibits modified phase behaviour with reduced transition enthalpies and spatially heterogeneous freezing processes, while alkanes and other molecular solids display confinement-induced crystallization and polymorphism.

Despite these significant modifications, a thermodynamic phase transition generally remains observable in all previously reported systems, albeit shifted in temperature or broadened in character.

Within this broader context, confinement strategies have been extensively explored to manipulate the structure and phase behaviour of ionic liquids.[11–14]

For example, geometric confinement within nanostructures such as carbon nanotubes can induce crystallization of ionic liquids into alternative solid phases that do not exist in the bulk.[15]

Similarly, chemically mediated confinement in polymer networks, including ionogels, can promote ordering through specific intermolecular interactions.[16]

These studies demonstrate that confinement can stabilize ordered ionic states; however, in most cases, the emergence of crystallinity is accompanied by a significant reduction in molecular dynamics, consistent with the conventional trade-off between structural order and mobility. More recently, confinement-induced frustration has emerged as an important concept in soft matter systems. Single-chain confinement has been shown to broaden polymer relaxation processes over multiple length scales, while confinement-induced packing frustration can substantially modify polymer transport and rheological behaviour. These studies suggest that confinement may act not only as a geometric restriction but also as a mechanism for generating frustration-dominated energy landscapes.[17, 18]

Despite these advances, a key challenge remains unresolved: whether ionic liquids can be crystallized without completely suppressing their intrinsic dynamical freedom.

In particular, the realization of a structurally ordered ionic state that is not fully dynamically arrested has not been clearly established.

Poly(meta-benzamide) (pMBA) and related meta-linked aramids can be prepared by phase-change polymerization (PCP), forming highly ordered aramid crystals directly from a melt.[19–22]

Here, we address this challenge using phase-change polymerization (PCP) of meta-linked aramids, which form highly ordered networks directly from a melt.[19–22] By carrying out PCP in BMIM–PF6 and related ionic liquids, we show that meta-linked polymer architectures can template a frustration-stabilized ordered state in which long-range order persists without a detectable melting transition and residual ionic dynamics remain, and that this state can be realized in both crystalline and amorphous meta-linked hosts.

Results

In this work we focus on meta-linked aramid architectures as topologically frustrated hosts for ionic liquids. Our primary system is crystalline poly(meta-benzamide) (pMBA) prepared by phase-change polymerization (PCP) in the ionic liquid 1-butyl-3-methylimidazolium hexafluorophosphate (BMIM–PF_6), which yields highly ordered lamellar crystallites that incorporate the ionic liquid in situ as the polymer crystallizes. As a polymer-only reference, we also prepare neat pMBA by conducting PCP in a non-ionic high-boiling medium (dibenzyl toluene) under otherwise comparable conditions, providing a benchmark for the intrinsic crystallization behaviour of the host polymer in the absence of an ionic liquid. In addition, we examine a simple physical blend obtained by post-mixing preformed pMBA powder with bulk BMIM–PF_6 at the same ionic-liquid loading as the PCP-derived composites, in order to distinguish confinement effects generated during PCP from those arising from drying or simple mixing. To disentangle the roles of topology and crystallinity, we further investigate an amorphous meta-linked analogue, poly(meta-oxybenzamide) (pMOB), and a para-linked control, poly(para-benzamide) (pPBA), which forms highly ordered crystals but does not stabilize a crystalline BMIM–PF_6 phase under identical PCP conditions. Together, these systems allow us to isolate topology-controlled chemical confinement as the key parameter governing the emergence of the frustration-stabilized solid state.

1. **In-situ crystallization under confinement**

Phase-change polymerization (PCP) of poly(meta-benzamide) (pMBA) was carried out in an ionic liquid medium (BMIM–PF_6) at 200 °C, where the monomer forms a homogeneous liquid phase prior to polymerization. Upon heating, polymerization proceeds from the melt, and the resulting polymer crystallizes directly from the ionic liquid.

During this process, the growing pMBA crystals develop in situ within the ionic liquid environment, thereby imposing spatial confinement on the surrounding ionic species as the crystal forms. As a result, the ionic liquid becomes incorporated and confined within the polymer crystal matrix during crystallization.

Poly(meta-oxybenzamide) was prepared by a polycondensation route analogous to pMBA, but under conditions that yield an amorphous meta-linked aramid network rather than a crystalline lattice, providing a topologically similar yet structurally disordered host.

The resulting composite exhibits emergent sharp Bragg reflections at room temperature that are absent in bulk BMIM–PF_6, indicating the formation of a crystalline ionic-liquid phase within the pMBA matrix (Fig. 1a–c). The confined ionic phase exhibits distinct diffraction peaks at $2\theta \approx 20.0°$, 21.1°, 26.8°, 29.2°, and 39.5°, which are absent in bulk BMIM–PF_6, confirming the formation of a confinement-induced ordered state rather than residual bulk crystallization.

In contrast, control samples prepared by post-mixing bulk BMIM–PF_6 with preformed pMBA at identical loadings do not show these reflections (Fig. 1d), confirming that crystallization arises intrinsically from

the PCP-driven in situ confinement process rather than from drying or surface-induced effects.

This indicates that crystallization of the ionic liquid is induced during polymer crystal growth.

2. Lattice retention under repeated thermal cycling

Variable-temperature powder X-ray diffraction (VT-PXRD) was used to examine the stability of the confined ionic-liquid lattice during thermal cycling between room temperature and 320 °C (Fig. 2).

The principal reflections exhibit small and fully reversible shifts in 2θ with temperature, accompanied by only minor and reversible broadening of the full width at half maximum (FWHM).

Control experiments on neat pMBA without ionic liquid (Fig. S1) show only smooth thermal shifts of the polymer peaks and no additional reflections, confirming that the observed reversible peak evolution originates from the confined BMIM–PF_6 lattice rather than from structural changes in the polymer matrix.

Taken together, these results demonstrate that the confined ionic-liquid lattice remains intact throughout thermal cycling, retaining structural coherence without evidence of phase segregation or irreversible coarsening.

Importantly, the diffraction peaks associated with the pMBA matrix remain unchanged throughout the measurements, showing only smooth thermal shifts.

This indicates that the formation of the ionic crystalline-like phase does not perturb the underlying polymer structure, and that the observed diffraction features arise independently from the confined ionic liquid.

3. Thermodynamic signatures of the confined transition

Differential scanning calorimetry (DSC) shows that the pMBA/BMIM–PF_6 composite exhibits no endothermic signals from –40 °C to 350 °C, in stark contrast to bulk BMIM–PF_6, which displays a distinct low-temperature endothermic peak (Fig. 3a–c). Any residual phase transition, if present, must therefore be either substantially broadened or suppressed below the detection limit of conventional DSC, consistent with strong confinement-governed thermodynamics.

The complete absence of thermal transitions indicates that BMIM–PF_6 remains in a structurally ordered confined state throughout the entire temperature range. These characteristics are consistent with nucleation and melting processes governed by nanoscale confinement and corroborate the VT-PXRD results demonstrating reversible lattice retention under thermal cycling.

A key question is whether the absence of a detectable melting transition reflects simple vitrification or kinetic arrest under confinement. However, several observations argue against this interpretation.

From a thermodynamic standpoint, the absence of a detectable melting transition could in principle also arise from conventional vitrification or extreme supercooling of the ionic liquid. However, several observations are inconsistent with this scenario.

First, the confined BMIM–PF_6 phase exhibits sharp Bragg reflections with only modest, fully reversible broadening upon heating and cooling, whereas structural glasses typically show diffuse scattering and irreversible relaxation signatures.

Second, no calorimetric glass transition or enthalpic relaxation is observed between −40 °C and 350 °C within the sensitivity of our DSC measurements (≈0.1–0.2 $J\,g^{-1}\,K^{-1}$), even though bulk BMIM–PF_6 displays a clear low-temperature endotherm in the same instrument.

Third, the confined lattice responds reversibly to repeated thermal cycles and retains a finite ionic conductivity at 30 °C, indicating that the system preserves localized degrees of freedom rather than being fully kinetically frozen.

Taken together, these observations are inconsistent with both conventional vitrification and metastable supercooled states.

In this sense, we use the term “non-ergodic state” to denote a solid-like phase in which the system does not explore the full equilibrium ensemble on experimental time scales, yet maintains well-defined long-range correlations and residual dynamical modes. The topology-controlled frustration field imposed by the meta-linked polymer effectively truncates the accessible configuration space, preventing the ionic liquid from relaxing into either a fully periodic crystal or a conventional glass.

We therefore interpret the confined BMIM–PF_6 phase as a frustration-stabilized, non-ergodic solid distinct from both supercooled liquids and structurally homogeneous glasses.

Generality of the frustration-stabilized state in an amorphous meta-linked host

To test the generality of this frustration-stabilized solid state, we examined an amorphous meta-substituted analogue, poly(meta-oxybenzamide) (pMOB), as a host for BMIM–PF_6.
The pMOB/BMIM–PF_6 composite likewise exhibits broadened but distinct diffraction features that qualitatively resemble those of the pMBA system, despite the absence of long-range crystallinity in the polymer matrix (Fig. 4a).
Differential scanning calorimetry further shows no detectable melting transition across the entire temperature range investigated (Fig. 4b), confirming that the confined ionic phase remains in a thermally stable ordered state without bulk-like phase transitions, even when the host polymer is amorphous.

These observations demonstrate that the emergence of anisotropic ordering in the confined ionic phase is not contingent on crystallographic matching with a specific host lattice, but is governed more generally by meta-linked polymer architectures that impose frustration under phase-change conditions.

4. Thermal stability

Thermogravimetric analysis (TGA) of the pMBA/BMIM–PF_6 composite shows a gradual, intermediate mass-loss behaviour that differs from both neat pMBA and bulk BMIM–PF_6, whereas a simple physical mixture of pMBA and BMIM–PF_6 exhibits two distinct decomposition onsets corresponding to the individual components (Supplementary Fig. S2). These observations indicate that the ionic liquid is confined within the polymer matrix and does not behave as a separate bulk phase. Thermogravimetric analysis of the pMBA/BMIM–PF_6 composite reveals a single, intermediate onset of mass loss that is distinct from both neat pMBA and bulk BMIM–PF_6, consistent with a confined ionic phase rather than a simple superposition of the two components (Supplementary Fig. S2). From the relative mass loss attributable to BMIM–PF_6, we estimate that the ionic-liquid content in the pMBA composites is on the order of 10 wt%, in good agreement with the intensity of the ionic-lattice reflections in the PXRD patterns

5. Chemical integrity under confinement

Infrared spectroscopy (IR) was performed on samples subjected to a heating cycle up to 300 °C at a rate of 10 °C min^{-1} and subsequently cooled to room temperature, as well as on samples without any thermal history. The characteristic vibrational bands of the imidazolium cation and PF_6^- anion were preserved in both cases, with no evidence of thermal or chemical decomposition. In contrast, the amide bands of pMBA exhibit small but systematic frequency shifts compared with neat pMBA, indicating specific polymer–ion interactions under confinement (Fig. S3). The presence and chemical stability of BMIM–PF_6 were further supported by XRF analyses. Characteristic P Kα signals corresponding to PF_6^- were detected by XRF (Fig. S4), consistent with the IR results.

6. Ionic response at ambient temperature

Electrochemical impedance spectroscopy was employed to assess ionic transport in the pMBA/BMIM–PF_6 composite under blocking-electrode conditions at 30 °C.
As shown in Fig. 5, the Nyquist plot of the confined composite exhibits a well-defined high-frequency intercept, corresponding to an effective ionic conductivity of 3.7×10^{-5} S cm^{-1}.This value is substantially lower than that of bulk BMIM–PF_6 (1~3×10^{-3} S cm^{-1} at 25 °C)[4] yet clearly higher than that of neat pMBA and simple physical mixtures, for which no measurable ionic response is detected under the same conditions.

The measured conductivity is several orders of magnitude lower than that of bulk BMIM–PF_6, consistent with restricted ionic motion under confinement. These observations demonstrate that ionic motion is not completely arrested in the frustration-stabilized solid state, even though bulk-like melting is suppressed.

The origin of ionic transport in this frustration-stabilized state is unlikely to be explained by percolation through a bulk-like liquid network.

This conclusion is supported by multiple independent observations. First, simple physical mixtures of preformed pMBA with bulk BMIM–PF_6 at identical nominal loadings show no measurable conductivity

under the same conditions, excluding macroscopic percolation pathways formed by residual liquid in intergranular voids. Second, the PXRD patterns of the pMBA/BMIM–PF_6 composites do not display any reflections attributable to bulk crystalline BMIM–PF_6, and thermogravimetric analysis reveals a single, intermediate mass-loss step rather than separate decomposition events for polymer and ionic liquid, consistent with a confined, non-phase-separated ionic fraction.

Taken together, these results indicate that ionic transport occurs within a structurally constrained and macroscopically non-percolating environment imposed by topological confinement.

While macroscopic percolation through a bulk-like liquid network can be excluded based on control experiments, including the distinct thermogravimetric behaviour compared to simple physical mixtures (Supplementary Fig. S2), the presence of highly localized liquid-like regions at the nanoscale cannot be fully ruled out. Nevertheless, even in such a scenario, the transport must occur within a structurally constrained environment imposed by topological confinement, rather than through a continuous bulk liquid phase.

Within this framework, two limiting transport scenarios can be considered. In one limit, ions migrate via thermally assisted hopping within the ordered confined domains, where frustration gives rise to a sparse network of accessible pathways. Such hopping-type and relaxation-mediated transport mechanisms are broadly consistent with established descriptions of ion conduction in disordered solid ionic conductors. [24,25]

In the other limit, transport is dominated by a thin, quasi-liquid interfacial layer at the polymer/ionic-lattice boundary, whose connectivity is defined by the meta-linked confinement geometry.

The available data do not yet allow us to discriminate quantitatively between these mechanisms; however, in both cases the conduction pathway is inherently confined and does not rely on macroscopic liquid percolation.

Distinguishing between these mechanisms will require future studies combining frequency-resolved spectroscopy with spatially sensitive structural probes.

Discussion

At a broader conceptual level, this work suggests that the apparent coupling between crystallinity and ionic motion is not necessarily fundamental, but can be rationally decoupled through topology-controlled chemical confinement.

Polymer topology is shown to play a key role in governing the balance between translational order and residual degrees of freedom under confinement, enabling a structurally ordered ionic-liquid state that is not fully dynamically arrested.

This interpretation is consistent with the non-ergodic character of the confined state inferred from thermodynamic and transport measurements.

From a conceptual standpoint, the confined BMIM–PF_6 phase does not represent a conventional crystal nor a kinetically trapped melt, but rather a confinement-stabilized state in which degrees of freedom are selectively partitioned.

The pMBA matrix suppresses long-range translational motion through geometric confinement and lattice templating, while allowing residual degrees of freedom to persist within the frustration-dominated energy landscape imposed on the ionic system.

This separation weakens the otherwise rigid coupling between crystallinity and dynamical arrest, indicating that crystallographic order does not necessarily imply complete immobilization.

This behaviour can be understood as a consequence of frustration transfer during polymer crystallization.

As the pMBA matrix forms a crystalline framework through phase-change polymerization, the system is kinetically driven into a configuration that cannot fully relax to a global free-energy minimum.

This process is expected to generate a frustration-dominated energy landscape. Importantly, this energy landscape is not confined to the polymer itself, but is spatially propagated to the confined ionic liquid during the crystallization process.

As a result, the ionic liquid is constrained by an externally imposed non-equilibrium energy landscape, which restricts its accessible crystallization pathways and prevents the formation of a fully equilibrated crystalline phase.

Variable-temperature diffraction demonstrates reversible lattice retention far beyond the bulk melting range; differential scanning calorimetry reveals an absence of melting transitions from –40 °C to 350 °C; and infrared spectroscopy confirms chemical integrity and steady ionic loading across thermal cycling.

Together, these results consistently support a confinement-stabilized state in which crystallographic order persists without a detectable melting transition.

This qualitative change in ordering from bulk to rigid nanoconfinement and meta-polymer confinement is summarized schematically in Fig. 6, which contrasts disordered bulk BMIM–PF_6, a fully periodic 3D crystal in rigid cavities, and quasi-two-dimensional ordering under meta-linked polymer confinement.

This generality across crystalline pMBA and amorphous pMOB hosts shows that the key control parameter is not a particular host lattice, but the meta-linked polymer architecture itself, which acts as a programmable frustration field that shapes the energy landscape of the confined ionic liquid.

These findings go beyond a system-specific observation and point to a more general principle. We note that qualitatively similar diffraction features have been observed in other polymer systems under ongoing investigation in our group, such as polyimide- and polypeptide-based materials. Taken together with recent studies on confinement-induced packing frustration, single-chain confinement, and geometrically frustrated self-assembly, the present results support a broader view in which frustration operates as a general design principle for generating non-equilibrium ordered states in soft matter systems.[17,18,23]

While these observations are preliminary and not analysed in detail here, they are consistent with the notion that quasi-two-dimensional ordering may emerge more broadly in polymer–confined systems.

In this context, we reveal a general strategy for generating non-ergodic states through polymer-induced frustration under phase-change conditions.

Furthermore, the observed diffraction features are not consistent with any reported crystallographic structures of BMIM–PF_6, including those identified in confined systems (see Supporting Information of ref. [15]).

This further supports that the present phase does not correspond to a conventional crystalline state, but instead reflects a distinct form of structural ordering governed by a frustration-dominated energy landscape.

A quantitative comparison of diffraction features, including peak distributions and densities, is provided in Table S1.

Importantly, the diffraction peaks associated with the pMBA matrix remain unchanged throughout the VT-PXRD measurements, showing only smooth thermal shifts characteristic of the polymer lattice, without the emergence of additional reflections.

This indicates that the formation of the ionic crystalline-like phase does not perturb the underlying polymer structure, and that the observed diffraction features arise independently from the confined ionic liquid.

Thus, the polymer matrix acts as a structurally robust confinement field, imposing a frustration-dominated energy landscape without undergoing structural reorganization.

Chemically assisted confinement offers a complementary perspective: cellulose ionogels leverage competitive hydrogen bonding to strengthen cation–anion pairing, triggering reversible ionic-liquid crystallization and stiffness switching [16].

Our pMBA system likewise shows systematic amide-band shifts consistent with specific polymer–ion interactions, but differs in two crucial aspects—thermal durability at elevated temperatures and the persistence of localized degrees of freedom—suggesting that the pMBA interface not only templates

order but also sustains structurally constrained fluctuations. Specific interactions between meta-linked aramids and ionic liquids have also been reported in solution-phase studies of PMIA/ionic-liquid systems.[26]

The contrast between meta- and para-linked aramids provides direct evidence for the importance of chemical confinement.

While both pMBA and pPBA form highly ordered crystalline matrices under phase-change polymerization, only the meta-linked topology stabilizes a crystalline ionic-liquid phase.

In the para-linked system, no crystalline IL reflections are observed under otherwise identical conditions (Fig. S5).

If the observed behaviour were governed primarily by geometric constraints arising from polymer topology, a comparable degree of ordering would be expected for other highly ordered polymer matrices.

The absence of such ordering in the para-linked system therefore indicates that geometric differences alone are insufficient, and that the key factor lies in the generation and transfer of a frustration-dominated energy landscape during polymer crystallization.

This distinction suggests that the role of polymer topology is not simply to impose static geometric constraints, but to determine how frustration is generated and dynamically propagated during crystallization.

A plausible microscopic origin of this difference lies in the intrinsic chain geometry of the meta-linked polymer, which introduces kinks along the backbone.

These kinks are expected to generate additional packing constraints during crystallization, leading to a higher degree of structural frustration compared to the para-linked analogue.

Recent studies have shown that frustration generated under confined environments can profoundly alter structural organization and molecular dynamics in soft matter systems. In polymer nanocomposites, confinement-induced frustration modifies relaxation pathways across multiple length scales, whereas packing frustration generated around anisotropic nanoparticle architectures creates non-trivial transport behaviour despite strong local interactions.[17,18]

This behaviour is fundamentally distinct from conventional confinement effects, where geometric restriction modifies phase transitions but does not eliminate them.

In contrast, the absence of a detectable melting transition in the present system indicates that spatial confinement alone is insufficient, and that the governing factor is the frustration-dominated energy landscape generated during polymer crystallization.

An additional factor that may contribute to the observed behavior is the inherent frustration of the ionic liquid itself.

Ionic liquids are known to exhibit frustrated packing due to structural asymmetry and competing interactions, often preventing the formation of simple, well-ordered crystalline phases.

In the present system, such intrinsic frustration may couple with the frustration-dominated energy landscape imposed by the polymer matrix, further restricting the ability of the ionic liquid to relax into a fully equilibrated crystalline state.

This suggests that the emergence of the present non-equilibrium ordered state arises from the cooperative interplay between the intrinsic frustration of the ionic liquid and the externally imposed frustration field generated during polymer crystallization.

Exploring other intrinsically frustrated systems under similar confinement conditions would therefore provide a promising direction for future investigation.

A unified picture therefore emerges in which confinement operates through three coupled effects:

(i) geometric confinement by nanoscale polymer crystallites, restricting spatial degrees of freedom;

(ii) frustration transfer from the polymer crystallization process, imposing a non-equilibrium energy landscape on the ionic system; and

(iii) local interactions that modulate short-range ordering without determining the global structure.

Together, these effects enable a partial decoupling of crystallinity and dynamical arrest.

In conclusion, this work demonstrates that crystallinity and ionic mobility are not inherently incompatible, but can be decoupled through topology-controlled chemical confinement.

We note that the frustration-stabilized solid state is realized at modest ionic-liquid loadings (approximately 10 wt% in pMBA), suggesting that the essential features of the energy landscape are controlled more by topology and confinement than by the absolute amount of imbibed ionic liquid.

More broadly, these findings challenge the conventional paradigm that structural order necessarily suppresses molecular motion, and establish a general design principle for engineering ordered ionic materials with independently tunable structural and dynamical properties.

The coexistence of long-range order, the absence of detectable melting, and finite ionic conductivity at 30 °C indicates that the confined BMIM–PF_6 phase does not behave as a fully immobilized crystalline solid.

Although the microscopic origin of this transport—whether dominated by motion within the ordered domains or along interfacial regions—remains to be clarified, these results support the view that

topology-controlled confinement can weaken the conventional coupling between crystallinity and ionic mobility in ionic liquids.

Together with the finite ionic conductivity observed at ambient temperature, these findings indicate that the frustration-stabilized state retains residual ionic degrees of freedom despite its long-range structural order.

It is noteworthy that similar diffraction features are observed even when the polymer matrix lacks long-range crystallinity, suggesting that the observed structural ordering of the confined ionic liquid is not strictly dependent on the crystalline order of the host polymer.

This observation further supports the notion that the ionic structure is governed by an underlying energy landscape imposed by the confinement environment, rather than by specific crystallographic matching with the polymer lattice.

We note that the frustration-stabilized state persists upon hot-pressing into dense pellets for impedance measurements, indicating that the non-equilibrium ionic configuration is sufficiently robust to survive mechanical processing and may in future be exploited to tune composite properties through processing history.

Similar topology-controlled confinement strategies could, in principle, be extended to other frustrated degrees of freedom, such as mixed-valence states or conformational isomerism, thereby opening a broader route to stabilizing non-equilibrium configurations beyond ionic liquids.

Methods

Materials and sample preparation

Poly(m-benzamide) (pMBA)/ 1-butyl-3-methylimidazolium hexafluorophosphate (BMIM–PF_6) was prepared from *m*-aminobenzoic acid via a phase-change polymerization. 20wt% of monomer was first dissolved to form a homogeneous liquid phase in BMIM–PF_6, followed by polymerization at 200 °C for 24h. Upon completion, the resulting highly ordered polymer crystallized out of the melt and was isolated by filtration after cooling. For meta-linked aramids such as pMBA, molecular weight is usually assessed from intrinsic viscosity in concentrated sulfuric acid. In the present pMBA/BMIM–PF_6 composites, the presence of confined ionic liquid prevents the use of this protocol, so absolute molecular-weight values cannot be determined reliably and are therefore not reported.

Neat poly(m-benzamide) (pMBA) was prepared from *m*-acetamidobenzoic acid via a phase-change polymerization. 1wt% of monomer was first dissolved to form a homogeneous liquid phase in dibenzyl toluene, followed by polymerization at 340 °C for 8 h. Upon completion, the resulting highly ordered polymer crystallized out of the melt and was isolated by filtration after cooling. Intrinsic viscosities measured in 96 wt% sulfuric acid were 0.28 dL g^{-1} for pMBA-Cryst and 0.15 dL g^{-1} for pMBA-Amorph.

After synthesis, all powder samples were thoroughly washed with hot acetone to remove residual reagents and dried under vacuum at 200 °C for 10 h prior to characterization.

To confirm that crystalline BMIM–PF_6 does not arise from simple drying or concentration, a physical mixture was prepared by blending neat pMBA powder (preformed) with bulk BMIM–PF_6 at the same ionic-liquid loading as the PCP-derived composite.
The mixture was stirred at room temperature to ensure complete wetting of polymer particles, followed by drying under vacuum at 200 °C for 10 h. For preparation of the physical mixture samples, preformed pMBA powder was manually mixed with BMIM–PF_6 using a mortar and pestle at room temperature until a visually homogeneous state was obtained. The mixture was then subjected to the same vacuum drying conditions as the PCP-derived samples prior to characterization.

The ionic-liquid content in the pMBA/BMIM–PF_6 composites was estimated from the TGA mass-loss profiles by assigning the high-temperature residue to the pMBA matrix and the low-temperature volatile fraction to BMIM–PF_6. This analysis yields an IL loading of approximately 10 wt% for the pMBA composites, consistent with the nominal composition and the relative intensity of the ionic-lattice reflections in PXRD.

Synthesis of poly(meta-oxybenzamide) (pMOB).
Poly(meta-oxybenzamide) was synthesized by step-growth polycondensation of *m*-aminophenoxybenzoic acid (or the corresponding diacid chloride/diamine pair) under conditions analogous to those used for pMBA, followed by quenching and work-up designed to suppress crystallization during cooling. As a result, the as-prepared pMOB forms an amorphous meta-linked aramid network, in contrast to the highly crystalline pMBA obtained under phase-change polymerization conditions.

Powder X-ray diffraction (PXRD)

Phase information of the pMBA powder was further confirmed at room temperature via PXRD using a Rigaku RINT-TTR3 diffractometer with Cu Kα radiation, operated at 40 kV – 40 mA at various temperatures. Variable-temperature PXRD was subsequently performed under vacuum using a Rigaku SmartLab diffractometer operated at 45 kV – 200 mA with Cu Kα radiation equipped with an Anton Paar DCS500 cooling/heating stage.

Differential scanning calorimetry (DSC)

Differential scanning calorimetry (DSC) measurements were performed using a Mettler Toledo DSC1 instrument. DSC scans were conducted under nitrogen atmosphere from -40 °C to 350 °C at heating/cooling rate 5 °C min^{-1}. Tg was determined from the midpoint of the step change in heat flow (second heating).

Thermogravimetric analysis (TGA)

Thermogravimetric analysis (TGA) measurements were performed using a Netzsch STA449 F1 instrument and carried out under argon atmosphere from 25 °C up to 700 °C at heating/cooling rate 10 °C min^{-1}.

Infrared spectroscopy (IR)

IR spectra were collected on a Jasco FT/IR-4100 spectrometer in transmission mode for powder samples using KBr as a fixing medium (4000–400 cm^{-1}, 4 cm^{-1} resolution, 64 samples). Samples were measured before and after heating to 300 °C to evaluate chemical integrity of BMIM–PF_6 and polymer–ion interactions.

X-ray fluorescence (XRF) spectroscopy

X-ray fluorescence (XRF) spectra were collected on a Rigaku EDXL300 spectrometer (25-50 kV, 1 mA) to confirm the presence and elemental composition of the ionic liquid in the pMBA/BMIM–PF_6 composite. Powder samples were mounted on PTFE holders with a 5 mm aperture and a Prolene film window and measured under vacuum at room temperature. The spectra were analyzed to identify characteristic signals of phosphorus from the PF_6^- anion. Spectra collected before and after thermal treatment at 300 °C showed no detectable change in elemental composition, indicating retention of BMIM–PF_6 and its thermal stability under the applied conditions.

Electrochemical impedance spectroscopy (EIS)

Electrochemical impedance spectroscopy (EIS) was performed on compression-moulded pMBA/BMIM–PF_6 sheet specimens. The composite material was processed into free-standing circular films with a diameter of 10 mm and a thickness of approximately 0.4–0.5 mm.

For film preparation, the pMBA/BMIM–PF_6 material (without post-annealing) was placed between Kapton films (0.2 mm thickness) and compression-moulded between rigid plates under a uniaxial load of approximately 12 kN at 300 °C for 5 min, yielding mechanically robust and well-formed composite sheets suitable for impedance measurements.

EIS measurements were conducted by an external analytical service (JFE Techno-Research Corporation) using a frequency-response analyzer in a dedicated conductivity measurement setup. The circular composite sheet was sandwiched between stainless-steel (SUS) fixtures acting as blocking electrodes and mechanically constrained using three M6 bolts to ensure stable electrical contact and reproducible fixation of the specimen. Cell assembly and measurements were carried out under ambient atmosphere. The specimen was clamped between stainless-steel blocking electrodes under a uniaxial compressive load of 3 N, applied using calibrated bolts, to ensure stable and reproducible electrical contact during the measurement.

AC impedance spectra were recorded over a frequency range from 1 MHz to 10 mHz with an applied AC amplitude of 10 mV. Frequencies above 100 kHz were treated as reference data due to increased

measurement uncertainty. All measurements were performed at a controlled temperature of 30 °C. A single measurement was conducted for each specimen under the specified conditions.

The impedance response is presented in the form of Nyquist plots. Conductivity values were estimated from the high-frequency intercept for representative samples; detailed equivalent-circuit modelling was not performed. To assess the influence of electrode contact pressure, EIS measurements were performed at clamping loads of 3 N and 5 N. The resulting spectra and conductivity values were comparable, indicating that the measured conductivity was not strongly dependent on the applied contact pressure within this range.

Prior to each impedance measurement, the sample was held at the target temperature for at least 30 min to ensure thermal equilibration. All measurements were conducted under blocking-electrode conditions using stainless-steel electrodes, such that the observed impedance response reflects intrinsic ionic dynamics within the bulk composite rather than electrode reactions. Although measurements were carried out under ambient atmosphere, no evidence of moisture-induced degradation or instability was observed, as confirmed by the reproducibility of impedance spectra and complementary IR/XRF analyses.

Statistical analysis and reproducibility

Unless otherwise stated, reported values represent the mean of three independent measurements. Electrochemical impedance spectroscopy measurements were performed once for each specimen under each contact-pressure condition (3 N and 5 N).

Declarations

Funding

This work was supported by the RIKEN–Sumitomo Chemical collaborative research program.

Acknowledgements

We gratefully acknowledge Professor Junji Watanabe for his insightful advice encouraging us in this study. We also thank Dr. Kiyohiro Adachi and Michiko Tanaka for their valuable assistance with X-ray diffraction (XRD) and X-ray fluorescence (XRF) measurements. We thank JFE Techno-Research Corporation for technical support in electrochemical impedance measurements.

Author Contributions

S.O. conceived and supervised the project. S.O. and J.L. designed the experiments and analyzed the data. S.O. performed the synthesis and J.L. performed structural characterization and the crystallographic analysis of pMBAs. S.O. wrote the manuscript with input from all authors. All authors discussed the results and contributed to the final version of the manuscript.

Competing Interests

S.O. is an inventor on a patent application related to the materials described in this work. All other authors declare no competing interests.

Data Availability

All data supporting the findings of this study are available within the article and its Supplementary Information files. Additional raw data are available from the corresponding author upon reasonable request.

References

1. Plechkova, A. E. & Seddon, K. R. Ionic liquids: advanced solvents for emerging applications. Chem. Soc. Rev. 37, 123–150 (2008). https://doi.org/10.1039/B006677J
2. Hayes, R., Warr, G. G. & Atkin, R. Structure and nanostructure in ionic liquids. Chem. Rev. 115, 6357–6426 (2015). https://doi.org/10.1021/cr500411q
3. Armand, M., Endres, F., MacFarlane, D. R., Ohno, H. & Scrosati, B. Ionic-liquid materials for the electrochemical challenges of the future. Nat. Mater. 8, 621–629 (2009). https://doi.org/10.1038/nmat2448
4. Tokuda, H., Hayamizu, K., Ishii, K., Susan, M. A. B. H. & Watanabe, M. Physicochemical properties and structures of room-temperature ionic liquids. 1. Variation of anionic species. J. Phys. Chem. B 108, 16593–16600 (2004). https://doi.org/10.1021/jp0473462
5. Wasserscheid, P. & Welton, T. (eds.) Ionic Liquids in Synthesis, 2nd edn (Wiley-VCH, Weinheim, 2008). https://doi.org/10.1002/9783527621194
6. Dupont, J., de Souza, R. F. & Suarez, P. A. Z. Ionic liquid (molten salt) phase organometallic catalysis. Chem. Rev. 102, 3667–3692 (2002). https://doi.org/10.1021/cr010338r
7. MacFarlane, D. R. et al. Ionic liquids and their solid-state analogues as materials for energy generation and storage. Nat. Rev. Mater. 1, 15005 (2016). https://doi.org/10.1038/natrevmats.2015.5
8. Forsyth, M., Pringle, J. M. & MacFarlane, D. R. Ionic liquids and polymers: future platforms for advanced functional materials. Chem. Mater. 16, 3546–3552 (2004). https://doi.org/10.1021/cm049658h
9. Barsoukov, E. & Macdonald, J. R. (eds.) Impedance Spectroscopy: Theory, Experiment, and Applications, 2nd edn (Wiley, Hoboken, 2005). https://doi.org/10.1002/0471716243
10. Sangoro, J. R. & Kremer, F. Charge transport and glass dynamics in ionic liquids. Acc. Chem. Res. 45, 525–532 (2012). https://doi.org/10.1021/ar2002024

11. Alcoutlabi, A. & McKenna, G. B. Effects of confinement on material behaviour at the nanometre size scale. J. Phys.: Condens. Matter 17, R461–R524 (2005). https://doi.org/10.1088/0953-8984/17/15/R01
12. Cheng, S. Z. D. & Lotz, B. Enthalpy from disorder: polymer crystallization and morphology development. Prog. Polym. Sci. 30, 641–682 (2005). https://doi.org/10.1016/j.progpolymsci.2005.03.001
13. Gu, Y. & Li, G. Ionic liquids under nanoscale confinement. Chem. Soc. Rev. 41, 5907–5921 (2012). https://doi.org/10.1039/C2CS35114A
14. Huber, P. Soft matter in hard confinement: phase transition thermodynamics, structure, texture, diffusion and flow in nanoporous media. J. Phys.: Condens. Matter 27, 103102 (2015). https://doi.org/10.1088/0953-8984/27/10/103102
15. Chen, S., Wu, G., Sha, M. & Huang, S. Transition of ionic liquid [bmim][PF6] from liquid to high-melting-point crystal when confined in multi-walled carbon nanotubes. J. Am. Chem. Soc. 129, 2416–2417 (2007). https://doi.org/10.1021/ja067972c
16. Wang, S. et al. Cellulose-mediated ionic liquid crystallization enables tough-stiff switchable ionogels. Nat. Commun. 16, 9007 (2025). https://doi.org/10.1038/s41467-025-64061-2
17. Huang, J. et al. Full-scale polymer relaxation induced by single-chain confinement enhances mechanical stability of nanocomposites. Nat. Commun. 15, 6747 (2024). https://doi.org/10.1038/s41467-024-51187-y
18. Sarkar, J. et al. Nanotetrapods promote polymer flow through confinement-induced packing frustration. Nat. Commun. 16, 8550 (2025). https://doi.org/10.1038/s41467-025-63555-3
19. Okamoto, S., Llandro, J., Gibbons, A., Arfaoui, M., Hashizume, D. & Watanabe, J. Orthogonal staggered alignment of molecular chains in aramid whiskers: a game-changer for sustainable, high-performance composites. Macromol. Rapid Commun. 47, e00919 (2026). https://doi.org/10.1002/marc.202500919
20. Okamoto, S., Llandro, J., Ikeda, J. & Watanabe, J. Perpendicular chain orientation in poly(para-benzamide) single-crystal nanowhiskers for enhanced dispersibility. ACS Appl. Nano Mater. https://doi.org/10.1021/acsanm.6c00698 (2026).
21. Fujita, S., Koda, T., Fukumoto, H. & Ohno, H. Hydrogen bonding in ion-conducting polymer/ionic liquid systems. Chem. Lett. 32, 1204–1205 (2003). https://doi.org/10.1246/cl.2003.1204
22. Zhang, S., Sun, N., He, X., Lu, X. & Zhang, X. Physical properties of ionic liquids: database and evaluation. J. Phys. Chem. Ref. Data 35, 1475–1517 (2006). https://doi.org/10.1063/1.2204959
23. Tomazic, F. et al. Geometric Frustration Directs the Self-Assembly of Nanoparticles with Crystallized Ligand Bundles. arXiv:2509.23337 (2025).
24. Macdonald, J. R. Impedance spectroscopy: emphasizing solid electrolytes. Solid State Ionics 13, 147–149 (1984). https://doi.org/10.1016/0167-2738(84)90198-6
25. Funke, K. Jump relaxation model: a microscopic approach to ion transport in solids. Prog. Solid State Chem. 22, 111–195 (1993). https://doi.org/10.1016/0079-6786(93)90002-9

26. Winters, J., Dehaen, W. & Binnemans, K. Solvation structure of poly-m-phenyleneisophthalamide (PMIA) in ionic liquids. *Phys. Chem. Chem. Phys.* 21, 4053–4062 (2019). https://doi.org/10.1039/C8CP07041E

Figures

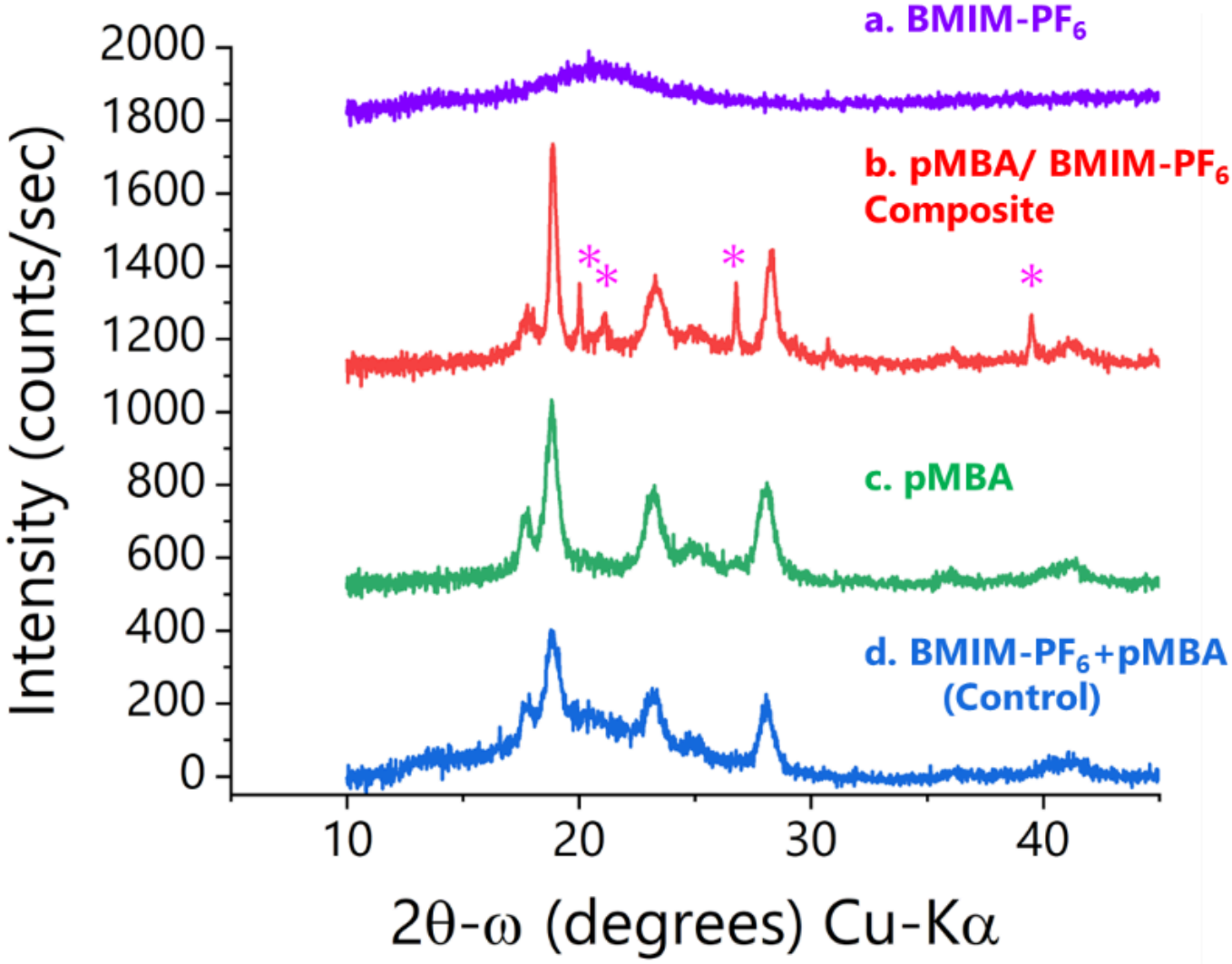

Figure 1

In-situ crystallization of BMIM–PF_6 within pMBA during phase-change polymerization.
a–c, Room-temperature PXRD patterns of bulk BMIM–PF_6, neat pMBA (prepared by PCP in dibenzyl toluene), and the PCP-derived pMBA/BMIM–PF_6 composite. The composite exhibits additional sharp Bragg reflections that are absent in both bulk BMIM–PF_6 and neat pMBA, indicating the formation of a confinement-induced crystalline ionic-liquid phase during PCP. d, PXRD pattern of a simple physical mixture of preformed pMBA and bulk BMIM–PF_6 at the same ionic-liquid loading as the PCP-derived composite. Only pMBA reflections are observed, with no Bragg peaks attributable to crystalline BMIM–PF_6, demonstrating that the ionic-lattice reflections in the composite arise uniquely from in-situ

confinement during PCP rather than from post-mixing or drying effects. These results establish that polymerization-driven confinement is essential for inducing the ordered ionic state.

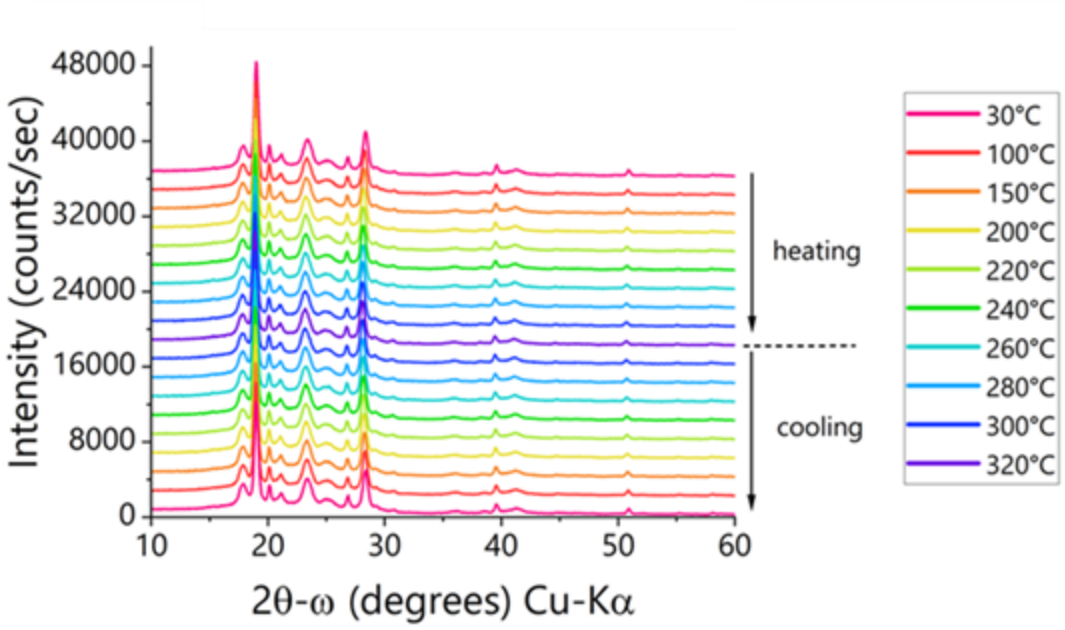

Figure 2

Thermally reversible retention of the confined BMIM–PF_6 lattice. Variable-temperature PXRD patterns of the pMBA/BMIM–PF_6 composite recorded between room temperature and 320 °C under vacuum. The confinement-induced ionic-lattice reflections persist throughout the entire temperature range and recover fully upon cooling, with only small, reversible shifts in 2θ and minor changes in peak width. No additional reflections associated with phase segregation or bulk-like melting are observed. In contrast, neat pMBA (Supplementary Fig. S1) shows only smooth thermal shifts of the polymer peaks, confirming that the evolving reflections in the composite originate from the confined ionic-liquid lattice rather than from structural changes in the host polymer. This reversible behaviour indicates that structural order is retained without irreversible relaxation, even at elevated temperatures.

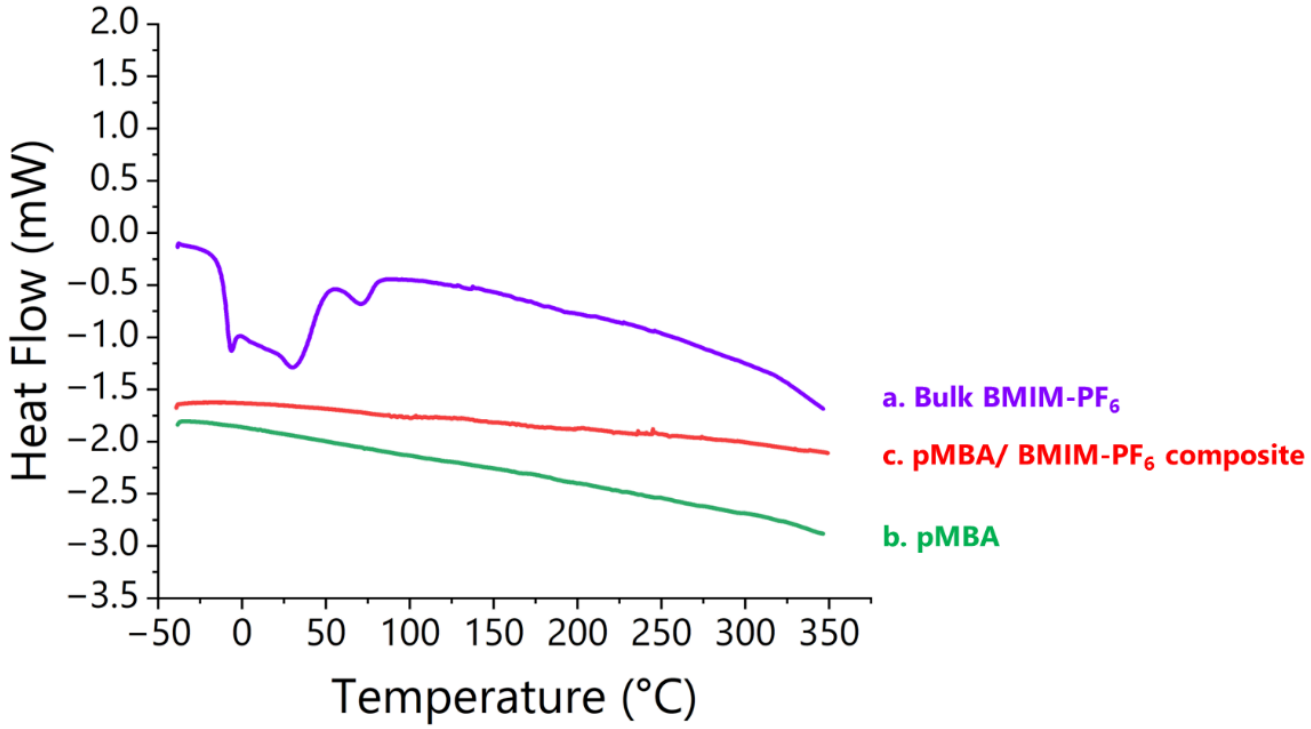

Figure 3

DSC evidence for the absence of bulk-like melting transitions in the confined ionic phase.

a–c, Differential scanning calorimetry (DSC) traces of bulk BMIM–PF_6, neat pMBA and the pMBA/BMIM–PF_6 composite recorded between −40 °C and 350 °C at 5 °C min^{-1} under nitrogen. Bulk BMIM–PF_6 exhibits a distinct endothermic transition from approximately −40 °C to 75 °C, whereas neat pMBA shows only its glass transition and polymer-related features. The composite displays no detectable endothermic events over the entire temperature range, despite the presence of long-range order in PXRD, indicating that the confined BMIM–PF_6 phase does not undergo a conventional bulk-like melting transition. The combination of DSC and VT-PXRD thus demonstrates that crystallographic order in the confined ionic phase persists without a thermodynamically defined melting point. This result provides direct thermodynamic evidence for an ordered state that does not undergo a conventional solid–liquid transition.

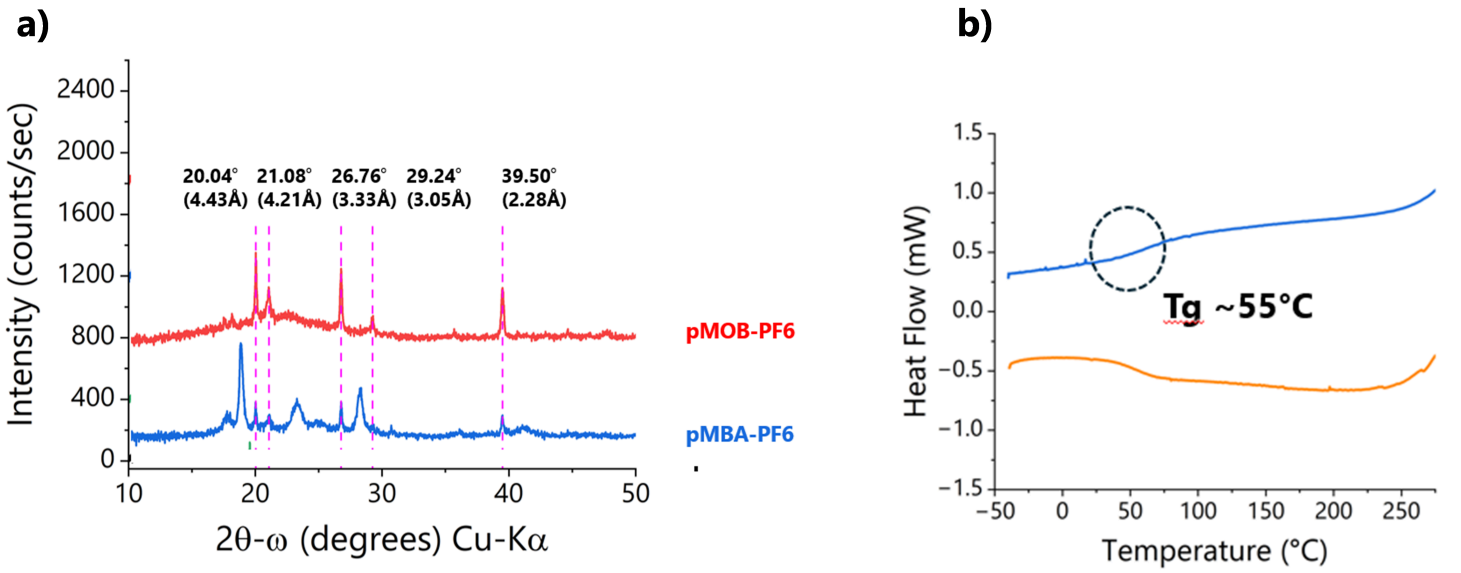

Figure 4

Frustration-stabilized solid state reproduced in an amorphous meta-linked host (pMOB). a, PXRD patterns of bulk BMIM–PF_6, neat pMOB and the pMOB/BMIM–PF_6 composite at room temperature. The composite shows broadened but distinct ionic-lattice reflections that qualitatively resemble those observed for the pMBA/BMIM–PF_6 system, despite the absence of long-range crystallinity in the pMOB matrix. b, DSC traces of bulk BMIM–PF_6, neat pMOB and the pMOB/BMIM–PF_6 composite. As in the pMBA system, the composite exhibits no detectable melting transition for the confined ionic phase over the investigated temperature range. These results demonstrate that the frustration-stabilized ionic phase exhibits diffraction features consistent with an ordered confined ionic phase. This establishes the generality of topology-controlled confinement as the governing principle.

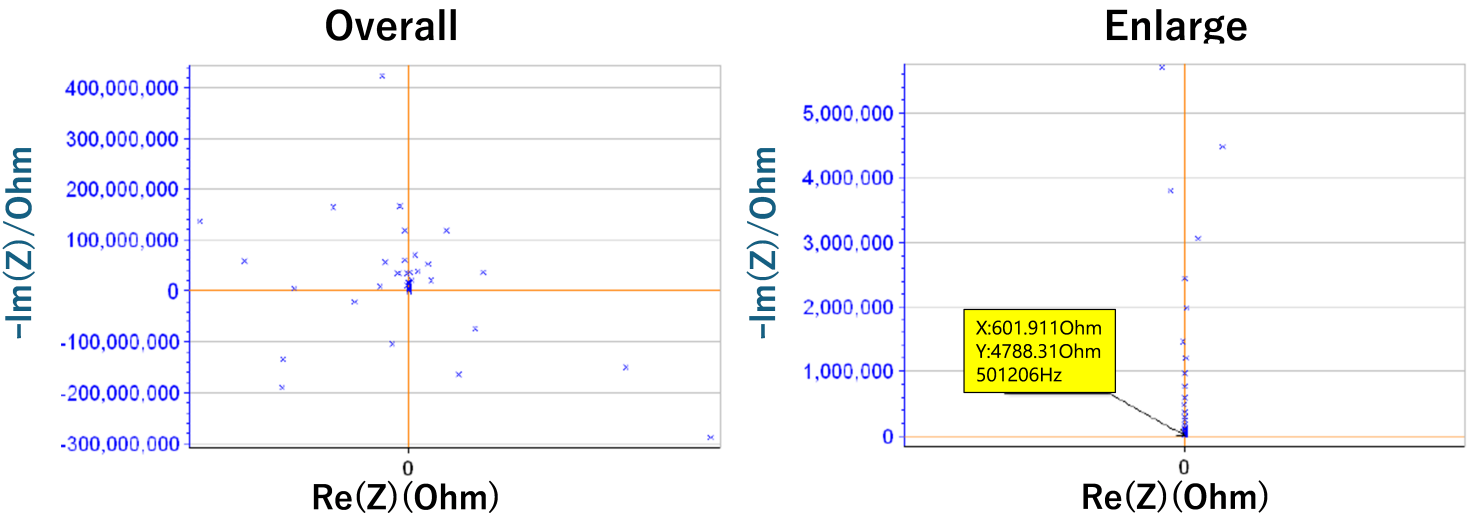

Figure 5

Solid-state ionic response of the confinement-stabilized BMIM–PF_6 phase.
Nyquist plot (left) and enlarged high-frequency region (right) of a compression-moulded pMBA/BMIM–PF_6 composite sheet (diameter ≈ 10 mm, thickness ≈ 0.4–0.5 mm) measured under blocking-electrode conditions with stainless-steel electrodes at 30 °C. The spectrum exhibits a depressed semicircle characteristic of an inhomogeneous ionic response. The high-frequency intercept corresponds to an effective ionic conductivity of approximately 3.7×10^{-5} S cm^{-1}, which is several orders of magnitude lower than that of bulk BMIM–PF_6 yet clearly higher than that of neat pMBA and simple physical mixtures, for which no measurable ionic response is detected under the same conditions. These observations show that ionic motion is not completely arrested in the frustration-stabilized solid state, even though bulk-like melting is suppressed, and confirm that the confined ionic phase retains residual dynamical degrees of freedom. This confirms that structural order and ionic mobility coexist within the confined state.

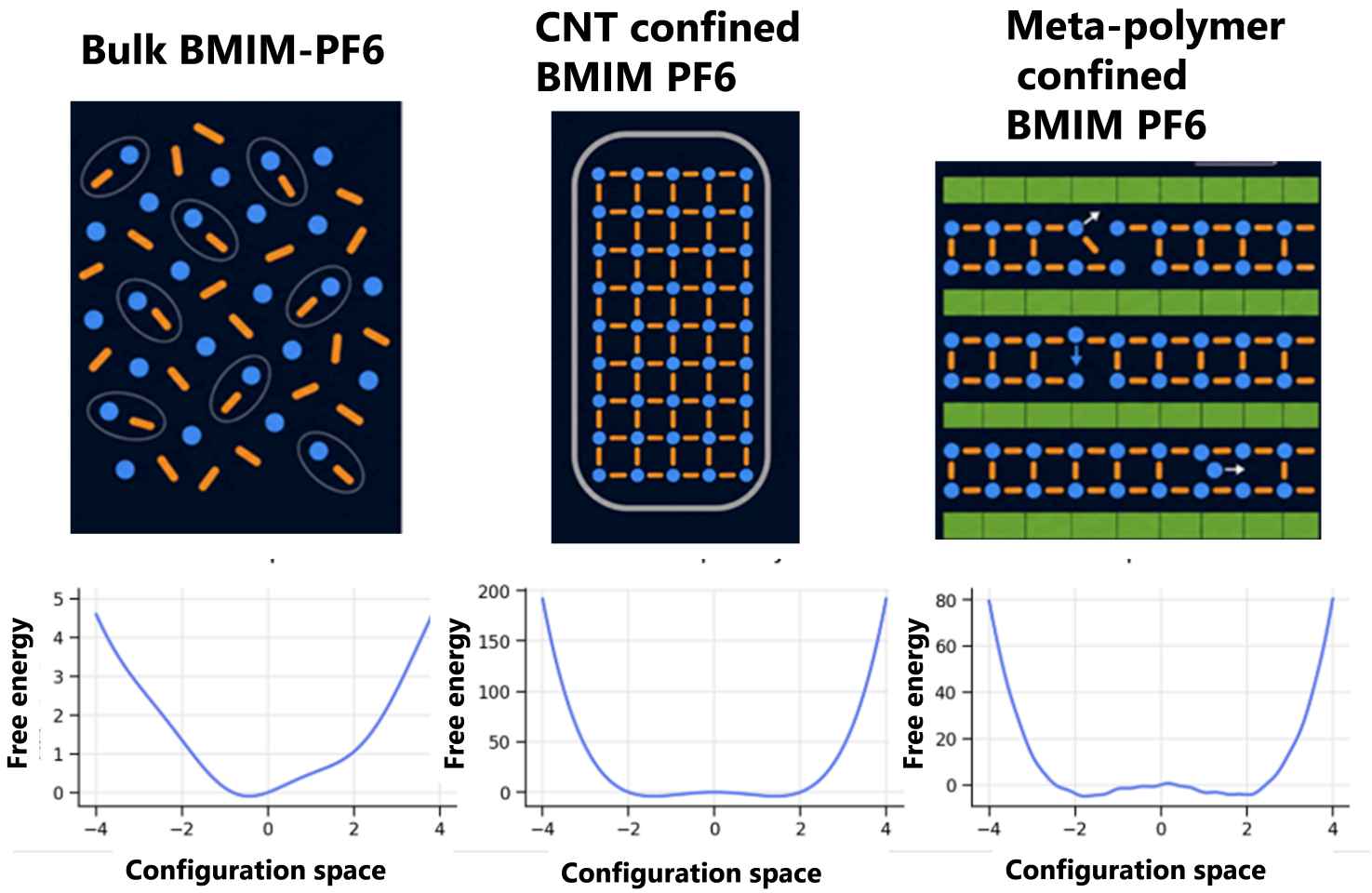

Figure 6

Real-space schematics of topology-controlled confinement in BMIM–PF_6.
Left, bulk BMIM–PF_6, in which cations and anions exhibit only short-range correlations without persistent long-range translational order.
Middle, BMIM–PF_6 confined within a rigid nanoscale cavity (for example, a carbon nanotube), where the ions assemble into a fully periodic three-dimensional crystalline arrangement.

Right, BMIM–PF_6 confined within a meta-linked polymer host, where the polymer topology imposes anisotropic ionic ordering and geometric frustration, enabling long-range order to coexist with residual ionic mobility. This schematic illustrates a distinct thermodynamic regime in which frustration limits the development of fully periodic crystallographic order while preserving residual dynamics. In the meta-polymer case, crystalline pMBA nanodomains act as a rigid confinement field, while BMIM–PF_6 resides in inter-crystalline nanodomains, forming a layered frustrated solid state exhibiting anisotropic ionic ordering. The accompanying energy-landscape schematics are illustrative and intended to convey the qualitative distinction between conventional crystalline ordering and frustration-stabilized confinement.

Supplementary Files

This is a list of supplementary files associated with this preprint. Click to download.

- SupportingInformation.docx